ISSN 0021-8944, Journal of Applied Mechanics and Technical Physics, 2015, Vol. 56, No. 6, pp. 977–983. © Pleiades Publishing, Ltd., 2015.
Original Russian Text © A.M. Bragov, L.A. Igumnov, V.B. Kaidalov, A.Yu. Konstantinov, D.A. Lapshin, A.K. Lomunov, F.M. Mitenkov.

EXPERIMENTAL STUDY AND MATHEMATICAL MODELING OF THE BEHAVIOR OF St.3, 20Kh13, AND 08Kh18N10T STEELS IN WIDE RANGES OF STRAIN RATES AND TEMPERATURES

A. M. Bragov[a], L. A. Igumnov[a], V. B. Kaidalov[b], A. Yu. Konstantinov[a], D. A. Lapshin[b], A. K. Lomunov[a, c], and F. M. Mitenkov[b]

UDC 539.3

Abstract: Results of an experimental study of the behavior of St.3, 20Kh13, and 08Kh18N10T steels under static and dynamic loading are reported. The influence of the strain rate and temperature on characteristics of strength and plasticity is studied. Based on the data obtained, the parameters of the Johnson–Cook model are determined. This model is used in commercial software to describe the yield surface radius as a function of loading parameters. The adequacy of the identified model is verified in a series of special test experiments.

Keywords: strain diagram, strain rate, adiabatic heating, Kolsky method, mathematical model, identification, verification.

DOI: 10.1134/S0021894415060073

INTRODUCTION

Numerical simulations of deformation and failure of containers designed for transportation of radioactive materials and their wastes require the use of mathematical models that provide an adequate description of the influence of loading conditions (strain rate and temperature) on straining of structural materials used to fabricate these containers. Various elements of these containers are made of 08Kh18N10T steel (main frame), 20Kh13 steel (fasteners), and St.3 steel (floor impacted by the container).

The present paper describes the results of an experimental study of the behavior of these steel brands for different strain rates and temperatures. The mechanical properties of steel under high-rate loading are determined by the Kolsky method with the use of the split Hopkinson bar. Based on strain diagrams constructed for different loading modes, the strength limits and their dependences on the strain rate and temperature are determined. To estimate the changes in strength in a wide range of strain rates, the results of dynamic experiments are compared with the results of similar static tests. Based on the resultant mechanical characteristics, the parameters of the Johnson–Cook plasticity model are determined for each steel brand by using the LS-DYNA software package with due allowance for the influence of the strain rate and temperature on the yield surface radius. Special test experiments are performed for verification of the mathematical model.

[a]Research Institute for Mechanics at the Lobachevsky State University of Nizhni Novgorod, Nizhny Novgorod, 603950 Russia; bragov@mech.unn.ru; igumnov@mech.unn.ru; constantinov.al@yandex.ru. [b]Afrikantov Experimental Design Bureau for Mechanical Engineering, Nizhnii Novgorod, 603074 Russia; kaidalov@mail.ru; lapshane@mail.ru; mitenkov_fm@mail.ru. [c]Nizhny Novgorod State University of Architecture and Civil Engineering, Nizhny Novgorod, 603950 Russia; lomunov@mech.unn.ru. Translated from Prikladnaya Mekhanika i Tekhnicheskaya Fizika, Vol. 56, No. 6, pp. 51–58, November–December, 2015. Original article submitted June 8, 2015.

METHODS OF THE EXPERIMENTAL STUDY

The Kolsky method [1–3] is used in this work to determine the characteristics of the materials under dynamic loading, and the Nicholas scheme [4] is used to find the characteristics of the materials under dynamic tension.

The behavior of the materials at temperatures up to 350°C was studied in a tubular furnace structure placed on the end faces of measuring bars with the steel specimen located between them. The specimen temperature was monitored by a chromel–copel thermocouple welded to the side surface of the specimen.

Repeated tests were performed for each loading mode (strain rate and temperature). Based on the series of diagrams, the averaged curve with confidence intervals characterizing the scatter of experimental data was determined for each test regime.

The error of determining the stress by the Kolsky method was within 7%, and the error of determining the specimen strain was smaller than 6% [5].

RESULTS OF EXPERIMENTAL INVESTIGATIONS

The conducted experiments showed that the yield stress of all examined steel brands increases with increasing strain rate and decreases with increasing temperature. The stress in the case of dynamic straining of St.3 steel (with the strain rate $\dot{\varepsilon} \sim 1000$ s^{-1}) is greater by 66% than that in the case of static straining; the corresponding values for 20Kh13 and 08Kh18N10T steels are 33 and 8%, respectively. When the steel specimens were heated to 350°C, the yield stress decreased by 24% for St.3 steel, 23% for 20Kh13 steel, and 20% for 08Kh18N10T steel. The limiting characteristics of plasticity (relative elongation δ and relative contraction ψ after fracture) are almost independent of the strain rate and temperature; the corresponding values are $\delta \approx 45\%$ and $\psi \approx 68\%$ for St.3 steel, $\delta \approx 32\%$ and $\psi \approx 65\%$ for 20Kh13 steel, and $\delta \approx 50\%$ and $\psi \approx 70\%$ for 08Kh18N10T steel.

IDENTIFICATION OF MATHEMATICAL MODELS

Based on the results of experimental investigations of the behavior of St.3, 20Kh13, and 08Kh18N10T steels under static and dynamic loading, we determined the parameters of the Johnson–Cook model. The yield stress is determined as a function of the strain, strain rate, and temperature [6]:

$$\sigma_{\rm JC} = (A + B\varepsilon_p^n)(1 + C\ln\dot{\varepsilon}^*)(1 - T^{*m}). \tag{1}$$

Here A, B, C, n, and m are the material parameters, ε_p is the effective plastic strain, $\dot{\varepsilon}^* = \dot{\varepsilon}/\dot{\varepsilon}_0$ is the dimensionless plastic strain rate ($\dot{\varepsilon}_0 = 1$ s^{-1}), $T^* = (T - T_0)/(T_m - T_0)$ is the modified homological temperature, $T_0 = 293$ K is the ambient temperature, and $T_m = 1723$ K is the melting point of the material.

The change in the material temperature due to the work of the plastic strain (adiabatic heating) is calculated by the formula

$$\Delta T = 0.9W_p/(\rho C_p),$$

where W_p is the work of the plastic strain, ρ is the material density, and C_p is the specific hear at constant pressure.

In addition to the linear (in terms of the strain rate logarithm) factor $1 + C\ln\dot{\varepsilon}^*$ in Eq. (1) (model 1), we considered other factors, which take into account the influence of the strain rate on the yield stress: $1 + C\ln(\dot{\varepsilon}^*) + C_2\ln(\dot{\varepsilon}^*)^2$ (model 2) [7], $(\dot{\varepsilon}^*)^C$ (model 3) [8], and $1 + (\dot{\varepsilon}^*/C)^{1/p}$ (model 4) [9]. Here C_2 and p are the material parameters.

The following characteristics of the examined steel brands were used in these models: $\rho = 7850$ kg/m^3, Young's modulus $E = 200$ GPa, Poisson's ratio $\nu = 0.28$, shear modulus $G = 78$ GPa, and $C_p = 462$ J/(kg·K).

The model parameters obtained by solving the optimization problem are listed in Tables 1–3. The best approximation (minimum deviation of the predicted curve from the experimental strain diagrams) for St.3 steel is obtained by using model 1; the best approximations for 20Kh13 and 08KH18N10T steels are provided by model 4. Figure 1 shows the strain curves calculated by the models that ensure the best fitting of the experimental data and also the experimental strain diagrams obtained for different loading conditions.

Table 1. Model parameters for St.3 steel

Model	A, MPa	B, MPa	n	C	C_2	p	m
1	412.5	1201	0.83	$2.18 \cdot 10^{-2}$	—	—	0.999
2	394.0	1136	0.83	$1.74 \cdot 10^{-2}$	0.00184	—	0.983
3	412.0	1223	0.83	$2.00 \cdot 10^{-2}$	—	—	0.996
4	192.0	570	0.83	$3.61 \cdot 10^{-2}$	—	26.758	0.993

Table 2. Model parameters for 20Kh13 steel

Model	A, MPa	B, MPa	n	C	C_2	p	m
1	611	956.5	0.4090	$1.26 \cdot 10^{-2}$	—	—	1.010
2	541	754.0	0.3978	$1.03 \cdot 10^{-2}$	0.00407	—	0.964
3	609	951.9	0.4096	$1.27 \cdot 10^{-2}$	0	—	1.008
4	611	708.0	0.3700	$5.56 \cdot 10^{3}$	—	0.9077	0.877

Table 3. Model parameters for 08Kh18N10T steel

Model	A, MPa	B, MPa	n	C	C_2	p	m
1	248.8	1339	0.6939	$8.18 \cdot 10^{-3}$	—	—	1.180
2	244.0	1338	0.7130	$7.49 \cdot 10^{-3}$	0.000822	—	1.164
3	249.0	1339	0.6950	$8.18 \cdot 10^{-3}$	—	—	1.179
4	120.0	648	0.6958	$1.53 \cdot 10^{-2}$	—	63.288	1.178

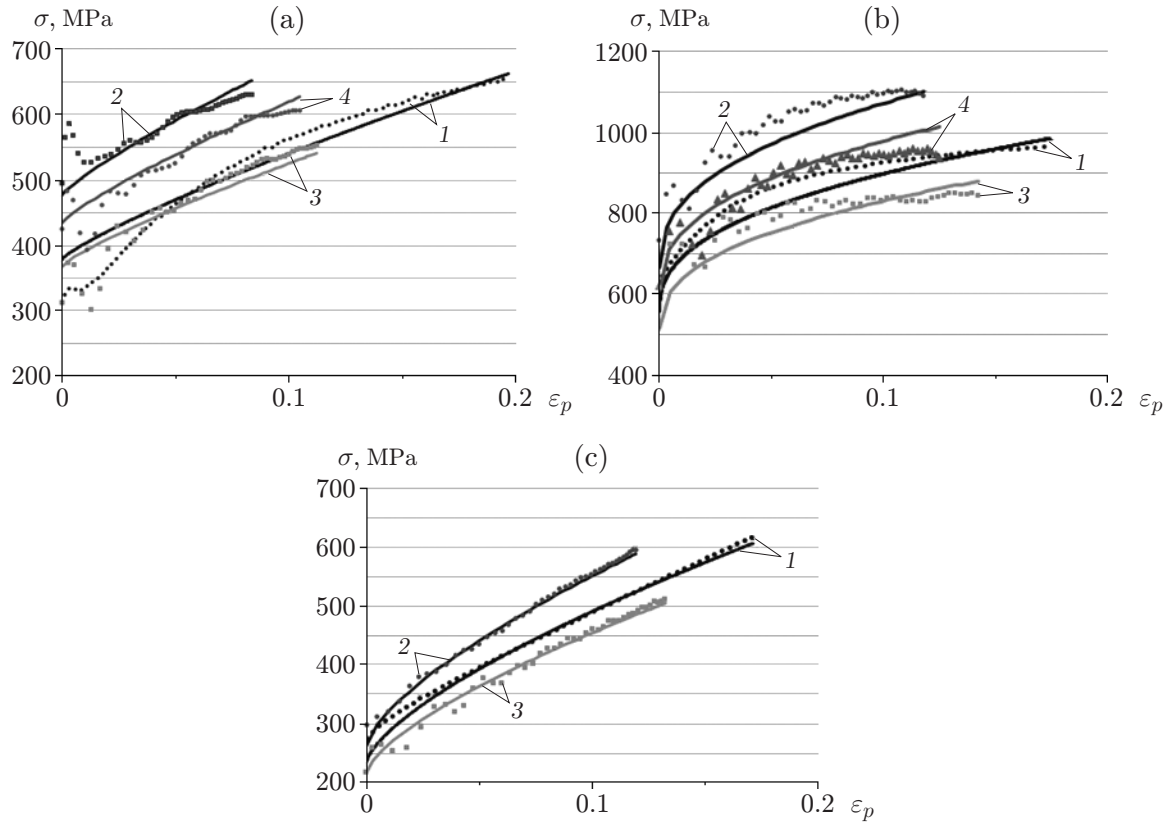

Fig. 1. Diagrams of static straining (*1*) and dynamic straining (*2–4*) of steel specimens: (a) St.3 steel; (b) 20Kh13 steel; (c) 08Kh18N10T steel; T = 20 (*1* and *2*), 350 (*3*), and 150°C (*4*); the curves and points show the model predictions and the experimental data, respectively.

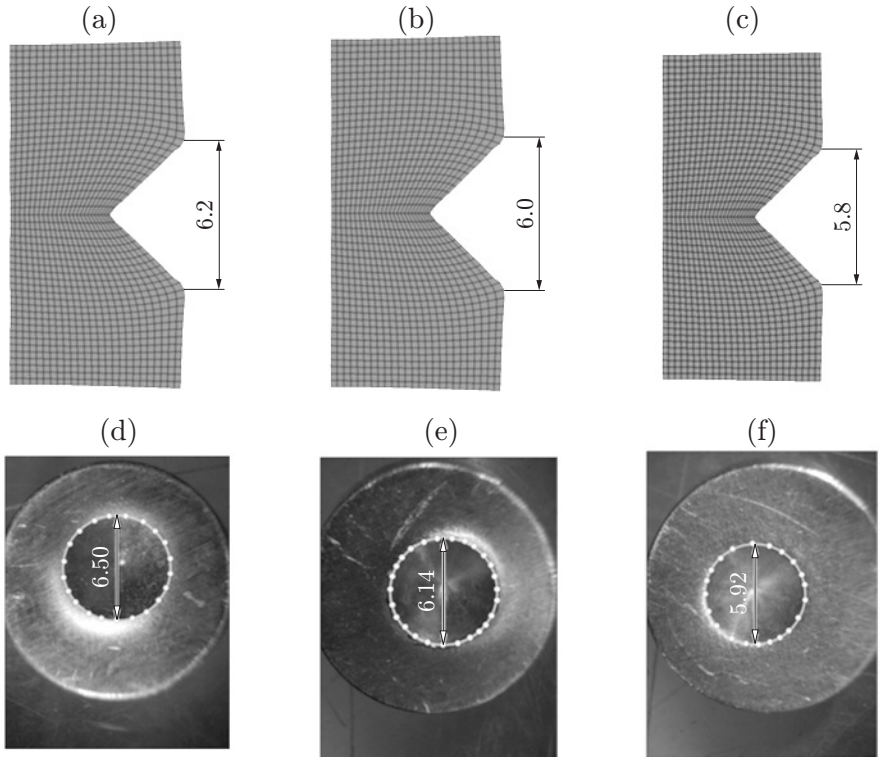

Fig. 2. Plastic footprints obtained in the numerical (a–c) and physical (d–f) experiments with penetration of the conical indentor into steel specimens: (a, d) St. 3 steel; (b, e) 20Kh13 steel; (c, f) 08Kh18N10T steel.

VERIFICATION OF MODELS OF STEEL STRAINING

As identification of mathematical models is based on results of simple (basic) experiments (homogeneous uniaxial stress state and constant strain rate and temperature), it is necessary to check whether the constitutive relations are valid for real conditions of operation of structural units. The stress–strain state in these elements is not homogeneous and uniaxial, and the strain rate can significantly change in the course of loading. Verification of model adequacy is performed in special test experiments, which are sufficiently simple and ensure a unique interpretation of results and numerical reproduction without simplifications. At the same time, the stress state and the character of variation of the loading parameters in test and basic experiments are different.

For verification of steel straining models, we performed experiments with high-velocity penetration of indentors with spherical and conical head parts into specimens made of the examined materials [10, 11] and with compression of the specimens over their diameters. In the first verification experiment, the indentor with the specimen were located in the split bar system and were loaded by a projectile flying with a certain velocity. The strains in the cross sections of the loading and support bars were recorded during the experiment, and the characteristic sizes of the plastic footprint in the specimen were measured.

In the second verification experiment (dynamic compression of the specimen over its diameter), we used a cylindrical specimen shaped as a pellet, which was turned in such a way that it was loaded over its diameter plane. The specimen loading pattern is similar to the test pattern used for splitting [12]. As in the first experiment, the strain gauges located on the measuring bars recorded the strain pulses. This information and also the data on the final shape of the specimen were used for verification of the models of the elastoplastic behavior of the materials.

The specimens were loaded in the split bar system with a diameter of 20 mm, which was made of high-strength steel. The steel projectile 20 mm in diameter and 300 mm long was accelerated to a velocity of 18.3 m/s in the case of penetration of the conical indentor and 22.4 m/s in the cases of the spherical indentor and compression over the specimen diameter.

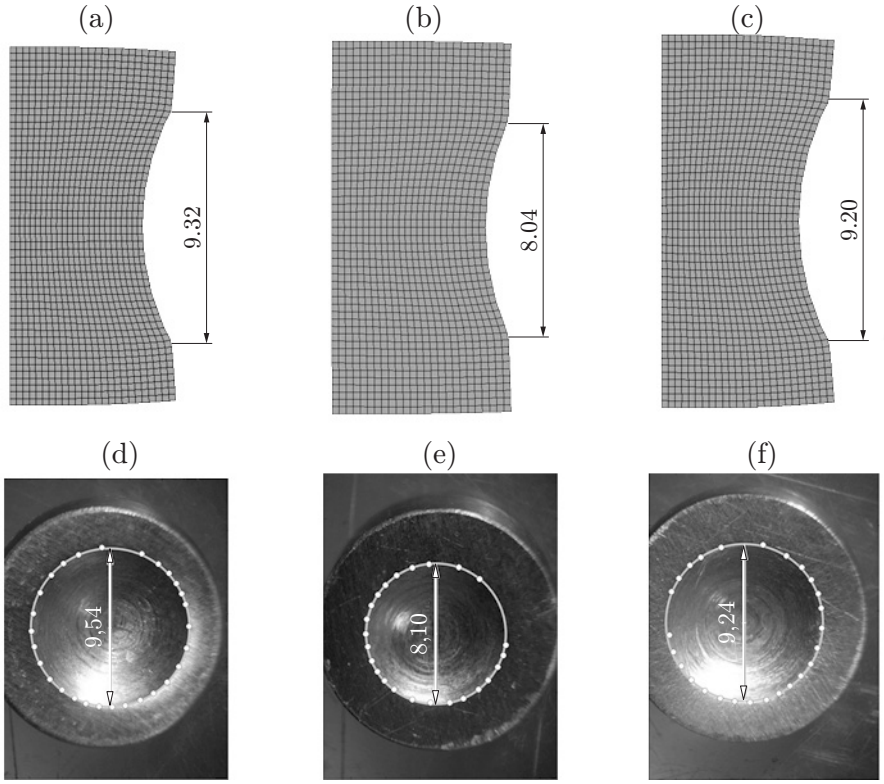

Fig. 3. Plastic footprints obtained in the numerical (a–c) and physical (d–f) experiments with penetration of the spherical indentor into steel specimens: (a, d) St.3 steel; (b, e) 20Kh13 steel; (c, f) 08Kh18N10T steel.

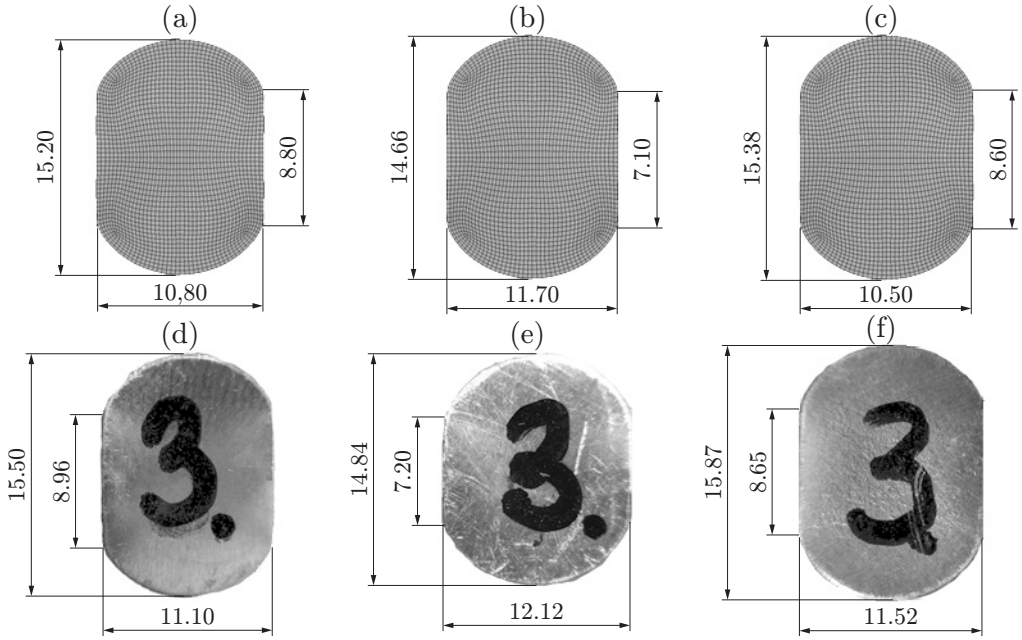

Fig. 4. Shapes of the computed (a–c) and experimental (d–f) specimens obtained from different steel brands: (a, d) St.3 steel; (b, e) 20Kh13 steel; (c, f) 08Kh18N10T steel.

Simulations of the experimental results on high-velocity penetration took into account the friction in the region of the indentor–specimen contact (the friction coefficient was equal to 0.1). The computations were performed in a plane axisymmetric formulation in the case with indentors and in a three-dimensional formulation in the case of compression over the specimen diameter.

The indentor footprints obtained in physical and numerical experiments are shown in Figs. 2 and 3 for the cases with the conical and spherical indentors, respectively. In the case with the conical indentor, the error in calculating the footprint diameter was 4.6% for St.3 steel, 2.3% for 20Kh13 steel, and 3% for 08Kh18N10T steel. The corresponding errors in the case with the spherical indentor were 2% for St.3 steel and 1% for 20Kh13 and 08Kh18N10T steel brands.

Figure 4 shows the specimen shapes after their compression over the diameter, which were predicted by the models and measured in the physical experiments.

It should be noted that the relative deviation of the computed characteristic sizes from the measured values was approximately 3% for St.3 steel, 3.5% for 20Kh13 steel, and 9% for 08Kh18N10T steel.

As a whole, the results of verification of the examined straining models show that the results of physical and numerical experiments are in good agreement in terms of both the final shapes of the specimens and the time characteristics of the plastic deformation process.

CONCLUSIONS

Strain diagrams under compression and tension were obtained in experiments with specimens made of St.3, 29Kh13, and 08Kh18N10T steel brands. It was noted that the dependences of the yield stress on the strain rate and temperature are different for these steel brands. Mathematical models from the LS-DYNA software package were identified for the examined materials on the basis of results of a series of static and dynamic tests at different temperatures. These models were verified in test experiments with high-velocity penetration of conical and spherical indentors and also in experiments with dynamic compression of the specimen over its diameter in the split bar system. Comparisons of the results of the physical and numerical experiments allows us to conclude that the mathematical models considered in this study produce reliable results for the examined materials and they can be used for analyzing the stress–strain state and strength of structural elements under dynamic loading.

This work was supported by the Russian Science Foundation (Grant No. 14-09-01096) and by the Ministry of Education and Sciences of the Russian Federation within the framework of the State Task (Grant No. 7.846.2014K).

REFERENCES

1. H. Kolsky, “An Investigation of the Mechanical Properties of Material at Very High Rates of Loading,” Proc. Phys. Soc. London **62B**, 676–700 (1949).
2. A. M. Bragov and A. K. Lomunov, “Peculiarities of Obtaining Stress–Strain Curves by the Kolsky Method,” in *Applied Problems of Strength and Plasticity (all-union collection of scientific papers)* (Gorkii University, Gorkii, 1984), pp. 125–137.
3. A. M. Bragov and A. K. Lomunov, “Methodological Aspects of Studying Dynamic Material Properties Using the Kolsky Method,” Int. J. Impact Eng. **16** (2), 321–330 (1995).
4. T. Nicholas, “Tensile Testing of Materials at High Rates of Strain,” Exp. Mech. **21** (5), 177–195 (1981).
5. A. M. Bragov, “Experimental Analysis of Processes of Deforming and Rupture of Materials at Strain Rate 10^2–10^5 s^{-1},” Doct. Dissertation in Tech. Sci. (Nizhny Novgorod, 1998).
6. G. R. Johnson and W. H. Cook, “A Constitutive Model and Data for Metals Subjected to Large Strains, High Strain Rates and High Temperatures,” in *Proc. of the 7th Int. Symp. on Ballistic, Hague (Netherlands), April 19–21, 1983* (Hague, 1983), pp. 541–547.
7. H. Huh and W. J. Kang, “Crash-Worthiness Assessment of Thin-Walled Structures with the High-Strength Steel Sheet,” Int. J. Vehicle Design **30** (1/2), 1–21 (2002).

8. D. J. Allen, W. K. Rule, and S. E. Jones, “Optimizing Material Strength Constants Numerically Extracted from Taylor Impact Data,” Exp. Mech. **37** (3), 333–338 (1997).
9. G. R. Cowper and P. S. Symonds, “Strain Hardening and Strain Rate Effects in the Impact Loading of Cantilever Beams,” Appl. Math. Rep. (Brown Univ., Providence, 1958).
10. A. Yu. Konstantinov, “Experimental-Computational Investigation of the Behavior of Structural Materials under Dynamic Loading,” Candidate’s Dissertation in Tech. Sci. (Nizhnii Novgorod, 2007).
11. V. L. Kotov, A. Yu. Konstantinov, Yu. I. Kibets, et al., “Numerical Modeling of Plane–Parallel Displacement of Conical Strikers in an Elastoplastic Medium,” Probl. Prochn. Plastichn. **75** (4), 303–311 (2013).
12. T. Rodriguez, C. Navarro, and V. Sanchez-Galvez, “Splitting Tests: an Alternative to Determine the Dynamic Tensile Strength of Ceramic Materials,” J. Physique IV **4**, 101–106 (1994).